INTERNATIONAL JOURNAL OF ADAPTIVE CONTROL AND SIGNAL PROCESSING
Int. J. Adapt. Control Signal Process. 2013; **27**:66–81
Published online 11 October 2012 in Wiley Online Library (wileyonlinelibrary.com). DOI: 10.1002/acs.2353

Adaptive range-measurement-based target pursuit

Barış Fidan [1,*,†], Soura Dasgupta [2] and Brian D. O. Anderson [3]

[1] *Department of Mechanical and Mechatronics Engineering, University of Waterloo, Canada*
[2] *Department of Electrical and Electronics Engineering, University of Iowa, USA*
[3] *Research School of Information Sciences and Engineering, Australian National University, Australia*

SUMMARY

This paper presents an adaptive scheme for localization of a target from distance measurements and motion control of a mobile agent to pursue this target. The localization and motion control task of interest is approached within a parameter-identifier-based adaptive control framework, where the localization is formulated as a parameter identification problem and the motion control is achieved using an adaptive controller based on the produced location estimates of the target. First, a robust adaptive law is designed to generate location estimate of the target using distance measurements. Then, following the standard certainty equivalence approach, a motion control law is developed considering substitution of the estimate generated by the localization algorithm for the unknown location of the target. Noting that there is some incompatibility between the persistence of excitation requirements of the localization algorithm and the target pursuit goal of the motion control law, the base motion control law is (re)designed to eliminate the effects of this incompatibility. The novelty of this paper is in this motion control design eliminating the persistence of excitation incompatibility. Stability and convergence analysis for the overall adaptive control scheme is presented. The results are valid in both two and three dimensions of motion space. The applications of the adaptive scheme include rescue localization, surveillance of signal sources, and formation acquisition of autonomous multi-robot/vehicle systems. Copyright © 2012 John Wiley & Sons, Ltd.

Received 13 September 2012; Accepted 17 September 2012

KEY WORDS: localization; target tracking; pursuit; adaptive control; persistence of excitation

1. INTRODUCTION

This paper deals with a simultaneous location estimation and motion control problem, bringing together two research fields, which recently have gained significant interest: *(cooperative) target localization* [1–5] and *target pursuit* [6–10]. Here, *target localization* refers to the process of estimating the precise location of a target by sensory agent(s) using information related to the relative position of the target, whereas the target can be another sensory agent cooperating with the pursuing sensory agent(s) or a separate entity to be captured. Leaving the cooperation and formation based target pursuit considerations for a follow-up work, in this paper, we focus on pursuit of a single target T by a single mobile agent A.

For this task, A needs measurements providing information about the relative position of the target. These measurements can be in different forms, including range, bearing, power level (indirectly related to distance) and time difference of arrival measurements [1, 3, 11, 12]. Although the general problem of interest for this paper could be studied in parallel approaches for different forms of such measurements, we will focus on the range measurement case only. In abstract terms, the problem of interest is the following:

*Correspondence to: Barış Fidan, MME Dept., University of Waterloo, 200 University Ave W., Waterloo, ON, N2L 3G1, Canada.
†E-mail: fidan@uwaterloo.ca

Problem 1.1
Given an agent A with position $y : \mathbb{R} \to \mathbb{R}^n$ as a function of time t, and a target T located at an unknown position $x \in \mathbb{R}^n$, $n \in \{2, 3\}$, devise a control law that uniformly achieves:

$$\lim_{t\to\infty} \|y(t) - x\| = 0,$$

using only the distance measurement,

$$D(t) = \|y(t) - x\|$$

and the agent's own position $y(t)$.

In the design of our adaptive localization and motion control scheme, we initially assume that the target T is stationary and the distance measurements are perfect; however, we subsequently consider possible effects of drifts in the position of T in our adaptive law design, and analyze the effects of such drifts as well as measurement noises.

Noting that the focus of the later sections of the paper is a mathematical systems design and analysis for solving problem 1.1 without considering the details of the real life implementation and application, next, we briefly discuss a means of real life implementation and application of an adaptive scheme that solves problem 1.1. Regarding implementation, the immediate question is how to obtain distance measurements. The distance measurements can be produced through various means. For example, if the target T emits a signal with known source signal strength Σ_T, the signal intensity and the characteristics of the medium provide a distance estimate for the agent A on the basis of the following relation:

$$s = \Sigma_T / d^{\eta},$$

where s is the received signal strength at A and η is the power loss coefficient for the particular environment. Alternatively, the agent A may transmit signals of its own, and estimate the distance by measuring the time it takes for such signals reflected off the target to return.

From the applications aspect, solving problem 1.1 is observed to have potential real-life applications in a number of areas including various localization and optimization tasks for mobile sensor networks [3,4], localization of emergency calls and rescue signal sources [3,13,14], localization of biological and chemical threats [3,15,16], localization of printers and other units in pervasive computing [3,17].

We approach problem 1.1 using a parameter identifier based adaptive control framework [18,19], where the localization of the target T by the mobile agent A is formulated as a parameter identification problem and a localization algorithm, in the form of a gradient adaptive law, is designed to produce the location estimates of T. The motion control of A is achieved using an adaptive controller on the basis of the produced location estimates. The motion control law design is designed in a way to move the mobile agent towards $\hat{x}$, the location estimate generated by the localization algorithm.

The *localization algorithm*, described in Section 2, permits the agent A to estimate the position x of T from measurements over an interval of $D(t)$, and is identical to a corresponding algorithm in [5,6]. The novelty of this paper is in the *adaptive control design* described in Section 3, noting that there is a *persistence of excitation* incompatibility between the localization and motion control tasks, and hence, the adaptive control design here is not a trivial one.

The paper also provides stability and convergence analysis of the proposed adaptive control scheme in Section 4 and a set of simulation results demonstrating the performance of the adaptive control scheme in Section 6. Concluding remarks are given in Section 7.

2. LOCALIZATION

In this section, we focus on the localization (parameter identification) part of the adaptive control approach to problem 1.1. The corresponding localization problem can be stated as follows:

DOI: 10.1002/acs

Problem 2.1
Given an agent A with position $y : \mathbb{R} \to \mathbb{R}^n$ as a function of time t, and a target T located at an unknown position $x \in \mathbb{R}^n$, $n \in \{2, 3\}$, devise an adaptive law to generate the estimate $\hat{x}(t)$ of x such that

$$\lim_{t\to\infty} \|\hat{x}(t) - x\| = 0, \tag{2.1}$$

using only the distance measurement,

$$D(t) = \|y(t) - x\| \tag{2.2}$$

and the agent's own position $y(t)$.

A gradient-type localization algorithm has already been designed in [5] to solve problem 2.1. To place the localization algorithm of [5] in the context of this paper, we note that [5] starts with the observation that because of (2.2), one obtains

$$\begin{aligned}\frac{\mathrm{d}}{\mathrm{d}t} D^2(t) &= 2\dot{y}^\top(t)(y(t) - x) \\ &= \frac{\mathrm{d}}{\mathrm{d}t}\|y(t)\|^2 - 2\dot{y}^\top(t)x,\end{aligned}$$

which, using the parameter identification framework of [18, 19], can be written in the linear parametric form

$$\bar{z}(t) = x^\top \bar{\phi}(t) \tag{2.3}$$

where

$$\bar{z} = \frac{1}{2}\frac{\mathrm{d}}{\mathrm{d}t}\left(\|y(t)\|^2 - D^2\right), \quad \bar{\phi} = \dot{y}.$$

Note here that, as in [5], the unknown position vector x is assumed to be constant. Nevertheless, the effect of drifts in x have been analyzed in [5], and similarly, the effects of such drifts to problem 1.1 will be discussed later in this paper.

With the parametric model (2.3), we propose the following *base* gradient algorithm to generate the estimate $\hat{x}$ of x:

$$\begin{aligned}\dot{\hat{x}}(t) &= \gamma\left(\bar{z}(t) - \hat{\bar{z}}(t)\right)\bar{\phi}(t), \\ \hat{\bar{z}}(t) &= \hat{x}^\top(t)\bar{\phi}(t)\end{aligned} \tag{2.4}$$

It is well known that in (2.4), $\hat{x}(t)$ converges exponentially to x, provided $\bar{\phi} = \dot{y}$ is *persistently exciting*, (*p.e.*), [18–20], with *p.e.* defined as follows:

Definition 2.1
[18–20] Consider any positive integer n and a signal $r : \mathbb{R} \to \mathbb{R}^n$. Then r is *p.e.* if there exist positive α_i and T_1, such that for all t, there holds

$$\alpha_1 I \leqslant \int_t^{t+T_1} r(\tau)r(\tau)^\top \mathrm{d}\tau \leqslant \alpha_2 I$$

Essentially, this requires that r persistently spans $\mathbb{R}^n$. The upper bound is simply a boundedness assumption. The α_i and T_1 will be called p.e. parameters. As shown in [5] for $n = 2$, $\dot{y}$ being p.e., is equivalent to the requirement that over every time interval of length T_1, the minimum distance of $y(\cdot)$ from any straight line be larger than a number that grows with α_1, that is, y persistently avoids a linear trajectory. Similarly, for $n = 3$, y must persistently avoid a planar trajectory. This accords with intuition as in $\mathbb{R}^2$, one must have distances from noncollinear points to achieve localization,

DOI: 10.1002/acs

just as in $\mathbb{R}^3$, one must have distances from noncoplanar points. Persistent avoidance of lines/planes stems from the need for exponential convergence.

Thus, (2.4) can serve as a localization step. *However its implementation requires generating the derivative of $D(t)$ rendering it impractical.* Instead, similarly to [5], we generate filtered versions of $\bar{z}$ and $\bar{\phi}$ using the set of equations set out as follows:

$$z(t) = \dot{\zeta}_1(t) = -\alpha\zeta_1(t) + \frac{1}{2}\left(y^\top(t)y(t) - D^2(t)\right), \tag{2.5}$$

$$\phi(t) = \dot{\zeta}_2(t) = -\alpha\zeta_2(t) + y(t), \tag{2.6}$$

where $\alpha > 0$, $\zeta_1(0)$ is an arbitrary scalar and $\zeta_2(0)$ is an arbitrary vector. Correspondingly, the revised parametric model and localization become, respectively,

$$z(\cdot) \equiv x^\top\phi(\cdot) \tag{2.7}$$

and

$$\begin{aligned}\dot{\hat{x}}(t) &= \gamma\left(z(t) - \hat{z}(t)\right)\phi(t),\\ \hat{z}(t) &= \hat{x}^\top(t)\phi(t),\end{aligned} \tag{2.8}$$

where for two functions f_1, f_2 we say $f_1(\cdot) \equiv f_2(\cdot)$ if there exist $\lambda, M > 0$ such that for all $t \geqslant 0$, $\|f_1(t) - f_2(t)\| \leqslant Me^{-\lambda t}$; $\gamma > 0$ is the adaptive gain and $\hat{x}(0)$ is the initial estimate.

Although the derivation of the parametric model (2.7) is a standard modeling procedure [18, 19], the formal derivation in our case follows immediately from the following lemma:

Lemma 2.1
Consider (2.2),(2.5) and (2.6), and assume that x is constant. Define

$$p(t) = x^\top\phi(t) - z(t) \tag{2.9}$$

and

$$\tilde{x}(t) = \hat{x}(t) - x. \tag{2.10}$$

Then there holds

$$\dot{p}(t) = -\alpha p(t) \tag{2.11}$$

and

$$\dot{\tilde{x}}(t) = -\gamma\phi(t)\phi^\top(t)\tilde{x}(t) - \gamma\phi(t)p(t). \tag{2.12}$$

Furthermore $\tilde{x}$ converges to zero exponentially if ϕ is p.e.

Proof
Taking derivatives of both sides of (2.5) and (2.6), we obtain

$$\dot{z}(t) = -\alpha z + \bar{z}(t) \tag{2.13}$$

$$\dot{\phi}(t) = -\alpha\phi(t) + \bar{\phi}(t) \;=\; -\alpha\phi(t) + \dot{y}(t) \tag{2.14}$$

Substituting in (2.3) leads to (2.11). Taking derivatives of both sides of (2.10) and substituting (2.8) and (2.9), we obtain (2.12).

Equation (2.11) implies that $p(t) \to 0$ exponentially as $t \to \infty$. This, together with definition 2.1 implies that, if ϕ is p.e., then the state $\tilde{x}$ of the linear time varying system 2.12 converges to zero exponentially. □

According to Lemma 2.1, exponential convergence of $\hat{x}$ to x is obtained as long as ϕ is p.e.. This in turn requires that $\dot{y}$ is p.e.. As will be evident in the sequel, the control objective of problem 1.1 is incompatible with a p.e. $\dot{y}$. The control law in the next section is partly motivated by this incompatibility.

DOI: 10.1002/acs

3. THE CONTROL LAW

We suggest the motion control law to be in the form

$$\dot{y}(t) = \dot{\hat{x}}(t) - \beta(y(t) - \hat{x}(t)) + f(D(t))\dot{\sigma}(t), \tag{3.1}$$

$$\dot{\sigma}(t) = A(t)\sigma(t), \tag{3.2}$$

where $\beta > 0$ is a design constant, and $f : \mathbb{R}^+ \to \mathbb{R}^+$ ($\mathbb{R}^+$ standing for $[0, \infty)$) and $A(\cdot) : \mathbb{R} \to \mathbb{R}^{n\times n}$ are to be selected such that they obey the following assumptions.

Assumption 3.1
The function $f : \mathbb{R}^+ \to \mathbb{R}^+$ is a strictly increasing, differentiable, bounded function that is zero at zero, and satisfies $f(D) \leqslant D,\ \forall D \in \mathbb{R}^+$.

Assumption 3.2

(i) There exists a $T > 0$ such that for all t,

$$A(t + T) = A(t), \tag{3.3}$$

and $A(t)$ is bounded.
(ii) $A(t)$ is skew symmetric for all t.
(iii) $A(t)$ is differentiable everywhere.
(iv) The derivative of σ in (3.2) is p.e. for any arbitrary nonzero value of $\sigma(0)$. More precisely, there exist positive $T_1, \alpha_i > 0$ such that for all $t \geqslant 0$ there holds

$$\alpha_1\|\sigma(0)\|^2 I \leqslant \int_t^{t+T_1} \dot{\sigma}(\tau)\dot{\sigma}(\tau)^\top \mathrm{d}\tau \leqslant \alpha_2\|\sigma(0)\|^2 I. \tag{3.4}$$

(v) For every $\theta \in \mathbb{R}^n$, and every $t \in \mathbb{R}^+$, there exists $t_1(t, \theta) \in [t, t + T_1]$, dependent on θ and t, such that $\theta^\top \dot{\sigma}(t_1(t, \theta)) = 0$.

We remark that [6] provides an $A(t)$ satisfying (i)–(iv) in Assumption 3.2 for $n \in \{2, 3\}$. That this same $A(t)$, which also satisfies (v), is shown in Section 5. Additionally, using (ii) of this assumption, [6] shows that σ has an additional important property:

Lemma 3.1
Consider (3.2) with $A(t)$ skew-symmetric. Then for all $t \geqslant 0$, $\|\sigma(t)\| = \|\sigma(0)\|$.

Having $A(t)$ bounded by Assumption 3.2 (i), Lemma 3.1 straightforwardly leads to the following corollary:

Corollary 3.1
Consider (3.2) with $A(t)$ satisfying Assumption 3.2. Then, there exists a finite number $\bar{\sigma}'$ such that for all $t \geqslant 0$, $\|\dot{\sigma}(t)\| \leqslant \bar{\sigma}'$.

The following assumption on the design constant β in 3.1 is further imposed for stability consideration that later appears in Section 4:

Assumption 3.3
The design constant β in 3.1 satisfies $\beta > \bar{\sigma}'$.

We conclude this section by motivating (3.1) and (3.2), and contrasting them to the corresponding step in the algorithm of [6]. First, observe from [5] that (2.5), (2.6) and (2.8) would achieve exponential localization, that is, drive $\hat{x}$ to x, if $\dot{y}$ were p.e.. The objective in [6] is to force y to

DOI: 10.1002/acs

asymptotically circumnavigate x at a specified *nonzero* distance from x, on a trajectory on which $\dot{y}$ is p.e.. The capturing or docking objective of problem 1.1, on the other hand, is fundamentally incompatible with $\dot{y}$ being p.e., as ultimately $\dot{y}$ must approach zero and therefore cannot be p.e.. It is however compatible with the more relaxed requirement that 'the degree of excitation', to coin a phrase, of $\dot{y}$ be large when y is far from x, and decline as y approaches x.

With this as background, we observe that the first two terms in the right hand side of (3.1), viewed in isolation from the third term, have the role of driving y to the estimated location $\hat{x}$ in a straight line. Should $\hat{x}$ converge to x then, of course, the convergence of y to $\hat{x}$ will ensure the convergence of y to x, accomplishing the control objective. What the third term in (3.1) does is to ensure that $\dot{y}$ is a signal with a degree of excitation that declines with D. In other words, when the docking objective is far from being met, $\dot{y}$ has a large degree of excitation. On the other hand, as the docking objective is approached, the degree of excitation declines correspondingly. Such a notion of an *objective driven excitation* to our knowledge is novel. Demonstrating its efficacy in assuring uniform asymptotic convergence, is a key contribution of this paper.

4. STABILITY AND CONVERGENCE ANALYSIS

This section shows that the closed loop systems defined in (2.2) and (2.5)–(3.2), globally, uniformly and asymptotically achieves the control objective of problem 1.1. In our analysis, instead of working with the original state vector $\left[\zeta_1, \zeta_2^\top, y^\top, \hat{x}^\top, \sigma^\top\right]^\top$, governed by (2.2) and (2.5)–(3.2), we work with the state vector

$$\mathcal{X} = [\phi^\top, y^\top, \tilde{x}^\top, p, \sigma^\top]^\top, \tag{4.1}$$

governed by (2.2), (2.10)–(2.12), (2.14), (3.1) and (3.2).

Observe that all elements of the original state space are bounded if this state vector is bounded. Further, the system governing this state space, and indeed the original, constitutes a *nonlinear periodic system*. Moreover, the essential impact of the variables ζ_i is captured by the introduction of ϕ, which is identical to $\dot{\zeta}_2$, and p, which captures important aspects of the error dynamics. Finally, the global objective, that is, that y should converge to x, is also demonstrated by working with $\mathcal{X}$. Noting, thus, that it suffices to work with this self contained new state space and its governing dynamics, Section 4.1 proves the boundedness of all signals appearing in the closed loop, and Section 4.2 proves global uniform asymptotic convergence.

4.1. Boundedness

As flagged earlier, we will now prove that $\mathcal{X}$ defined in (4.1) is bounded. To this end, we need the following Lemma.

Lemma 4.1
Consider $\rho : \mathbb{R} \to \mathbb{R}^n$ that obeys

$$\dot{\rho}(t) = -\left(\bar{\alpha} - g(t)\right)\rho(t) + \rho_0(t),$$

where $\bar{\alpha} > 0$, $\rho_0 : \mathbb{R} \to \mathbb{R}^n$ is bounded and $g : \mathbb{R} \to \mathbb{R}$ is in $\mathcal{L}_2$. Then, $\rho(.)$ is bounded.

Proof
First, consider the homogeneous system as follows:

$$\dot{\rho}_1(t) = -\left(\bar{\alpha} - g(t)\right)\rho_1(t). \tag{4.2}$$

Observe with $u(t) = \rho_1^2(t)/2$, there holds

$$\dot{u}(t) = -\left(\bar{\alpha} - g(t)\right)u(t) \leqslant -\left(\bar{\alpha} - |g(t)|\right)u(t). \tag{4.3}$$

By the Bellman–Gronwall inequality for all t_0 and $t \geqslant t_0$, we have

$$u(t) \leqslant u(t_0)e^{-\int_{t_0}^{t}(\bar{\alpha}-|g(s)|)ds} \tag{4.4}$$

DOI: 10.1002/acs

Because $g \in \mathcal{L}_2$, for every $\epsilon_1 > 0$, there is a t_0, such that for all $t > t_0$,

$$\int_{t_0}^{t} g^2(s)\mathrm{d}s < \epsilon_1.$$

Consequently, for $t \geqslant 1 + t_0$, by the Cauchy–Schwarz inequality, there holds

$$\int_{t_0}^{t} |g(s)|\mathrm{d}s < \sqrt{(t-t_0)\int_{t_0}^{t} g^2(s)\mathrm{d}s} < \sqrt{(t-t_0)\epsilon_1} \leqslant \sqrt{\epsilon_1}(t-t_0).$$

Thus, by choosing $\sqrt{\epsilon_1} < \bar{\alpha}$, one finds from (4.4) that (4.2) is exponentially stable, and the result follows because ρ_0 is bounded. □

Next, we show the boundedness of closed loop signals.

Theorem 4.1
Consider (2.2), (2.10)–(2.12), (2.14), (3.1) and (3.2), with Assumptions 3.1 and 3.2 in force. Then, $\mathcal{X}$ in (4.1) is bounded.

Proof
With $a > 0$, consider the nonnegative, Lyapunov like function:

$$L(t) = \frac{ap^2 + \|\tilde{x}\|^2}{2}, \tag{4.5}$$

with

$$a > \frac{\gamma}{4\alpha}. \tag{4.6}$$

Direct verification shows that

$$\dot{L}(t) = -\left(a\alpha - \frac{\gamma}{4}\right)p^2 - \gamma\left(\tilde{x}^\top(t)\phi(t) + \frac{p}{2}\right)^2. \tag{4.7}$$

Because of (4.6), $\dot{L}(t) \leqslant 0$. Thus, $\tilde{x}$ and p are bounded; and $\hat{x}$ is bounded. Further, because of Lemma 3.1 and Corollary 3.1, σ and $\dot{\sigma}$ are bounded. Moreover, because of Assumption 3.1, from (3.1), $y - \hat{x}$ and its derivative are bounded. Consequently, y is bounded. Using (2.14) and (3.1), there holds

$$\begin{aligned}\dot{\phi}(t) &= -\alpha\phi(t) + \dot{y}(t)\\ &= -\alpha\phi(t) + \dot{\hat{x}}(t) - \beta(y(t) - \hat{x}(t)) + f(D(t))\dot{\sigma}(t)\\ &= -(\alpha + \gamma e(t))\,\phi(t) + q(t)\end{aligned}$$

where $e(t) = \tilde{x}^\top(t)\phi(t) + p(t)$ and

$$q(t) = -\beta(y(t) - \hat{x}(t)) + f(D(t))\dot{\sigma}(t),$$

is bounded. From (4.7), $p, e \in \mathcal{L}_2$. Thus, from Lemma 4.1, $\phi(t)$ is bounded. □

4.2. *Uniform asymptotic convergence*

Next, the main result of convergence is presented.

Theorem 4.2
Consider (2.2), (2.10)–(2.12), (2.14), (3.1) and (3.2), with Assumptions 3.1–3.3 in force and let $\sigma(0) \neq 0$. Then, the following converges uniformly asymptotically to zero:

$$\left[\tilde{x}^\top(t), y^\top(t) - \hat{x}^\top(t), \phi^\top(t), p(t)\right]^\top.$$

DOI: 10.1002/acs

Proof

First, observe that the closed loop is periodic, and hence, convergence implies uniform convergence. We will invoke Lasalle's theorem. Consider the Lyapunov-like function in (4.5) with (4.6) in force.

Theorem 4.1 shows that L lies in a compact set. Thus, all signals converge to trajectories defined by

$$\dot{L} \equiv 0. \tag{4.8}$$

Under (4.6), and because of (4.7), this implies that $p \equiv 0$ and

$$\tilde{x}^{\top}(t)\phi(t) \equiv 0. \tag{4.9}$$

Because ϕ is bounded, from (2.12),

$$\dot{\tilde{x}}(t) \equiv 0. \tag{4.10}$$

In particular, there exists a constant $\tilde{x}^*$ such that

$$\tilde{x}(t) \equiv \tilde{x}^*. \tag{4.11}$$

We next assert that there holds

$$\tilde{x}^* = 0. \tag{4.12}$$

To see this, first observe that from (4.9) and (2.14), there holds

$$\begin{aligned} 0 &\equiv \tilde{x}^{*\top}\dot{\phi}(t) \\ &\equiv -\alpha\tilde{x}^{*\top}\phi(t) + \tilde{x}^{*\top}\dot{y}(t) \\ &\equiv \tilde{x}^{*\top}\dot{y}(t). \end{aligned}$$

Thus because of (2.10), (3.1) and (4.10),

$$\begin{aligned} 0 &\equiv \tilde{x}^{*\top}\dot{y}(t) \\ &\equiv \tilde{x}^{*\top}\left(\dot{y}(t) - \dot{\hat{x}}(t)\right) \end{aligned} \tag{4.13}$$

$$\equiv -\beta\tilde{x}^{*\top}\left(y(t) - \hat{x}(t)\right) + f(D(t))\tilde{x}^{*\top}\dot{\sigma}(t). \tag{4.14}$$

(4.13) and (4.14) further imply that

$$f(D(t))\tilde{x}^{*\top}\dot{\sigma}(t) \equiv \beta\tilde{x}^{*\top}\left(y(t) - \hat{x}(t)\right) \equiv \beta_1, \tag{4.15}$$

where β_1 is a constant. Because of (v) of Assumption 3.2, $\beta_1 = 0$, that is,

$$f(D(t))\tilde{x}^{*\top}\dot{\sigma}(t) \equiv 0. \tag{4.16}$$

To establish a contradiction, suppose (4.12) is false. Then Assumption 3.2 ensures that $\tilde{x}^{*\top}\dot{\sigma}(t)$ does not converge to zero. Thus, because of (4.16), $f(D(t)) \equiv 0$. Then, because of Assumption 3.1, $y(t) \equiv x$. Consequently, because of (4.14) and (4.16), (4.12) holds, establishing a contradiction.

It remains to show that along the trajectories defined by (4.8), $D(t)$ converges to 0.

Define $\Delta = y - x$ and $L_1 = \frac{\Delta^{\top}\Delta}{2}$. By (3.1), (2.12), (4.12), and Assumption 3.1 and we have that

$$\begin{aligned} \dot{L}_1 &= -2\beta L_1 + f\left(\|\Delta\|\right)\Delta^{\top}\dot{\sigma} \\ &\leqslant -2\beta L_1 + f\left(\|\Delta\|\right)\|\Delta\|\|\dot{\sigma}\| \\ &\leqslant -2\beta L_1 + \|\Delta\|^2\|\dot{\sigma}\| \\ &= -2\left(\beta - \|\dot{\sigma}\|\right)L_1. \end{aligned}$$

Then the result follows from Assumption 3.3. □

DOI: 10.1002/acs

5. SELECTION OF $A(T)$

Reference [6] presents a procedure for the selection of $A(t)$ that assures (i)–(iv) of Assumption 3.2 for $n \in \{2, 3\}$. In this section, we show that this same choice also satisfies (v) of Assumption 3.2 for $n \in \{2, 3\}$.

Consider first $n = 2$: With

$$E = \begin{bmatrix} 0 & 1 \\ -1 & 0 \end{bmatrix}, \tag{5.1}$$

the matrix

$$A(t) = aE, \quad a \in \{\mathbb{R} \setminus \{0\}\}, \tag{5.2}$$

has been shown in [6] to satisfy (i)–(iv) of Assumption 3.2 with

$$T_1 = \frac{\pi}{|a|}. \tag{5.3}$$

We now show that (5.2) satisfies (v) of Assumption 3.2 as well.

Theorem 5.1
With $\sigma : \mathbb{R} \to \mathbb{R}^2$ consider (3.2), with $A : \mathbb{R} \to \mathbb{R}^{2\times 2}$ as in (5.1) and (5.2). Then σ obeys (v) of Assumption 3.2 with T_1 as in (5.3).

Proof
With $\sigma(t) = [\sigma_1(t), \sigma_2(t)]^\top$, define $\psi(t)$ as

$$\psi(t) = \angle(\sigma_1(t) + \boldsymbol{j}\sigma_2(t)).$$

that is, the argument of the complex number $\sigma_1 + \boldsymbol{j}\sigma_2$. Then, as shown in [6], there holds for all $t \geqslant t_0 \geqslant 0$,

$$\sigma(t) = \|\sigma(t_0)\|[\cos(a(t - t_0) + \psi(t_0)), \sin(a(t - t_0) + \psi(t_0))]^\top,$$

that is,

$$\dot{\sigma}(t) = a\|\sigma(t_0)\|[-\sin(a(t - t_0) + \psi(t_0)), \cos(a(t - t_0) + \psi(t_0))]^\top,$$

Then, for every $\theta = [\theta_1, \theta_2]^\top \in \mathbb{R}^2$, with

$$\delta = \tan^{-1}\frac{\theta_1}{\theta_2}$$

there holds

$$\theta^\top\sigma(t) = a\|\sigma(t_0)\|\|\theta\|\cos(a(t - t_0) + \psi + \delta),$$

which must become zero over any interval of length T_1 defined in (5.3). □

For $n = 3$, the matrix $A(t)$ is defined in [6] as below. Effectively, $A(t)$ in this case switches periodically between the two 3×3 matrices

$$B = \begin{bmatrix} 0 & 0 \\ 0 & bE \end{bmatrix}, \text{ and} \tag{5.4}$$

$$C = \begin{bmatrix} cE & 0 \\ 0 & 0 \end{bmatrix} \tag{5.5}$$

DOI: 10.1002/acs

b and c being real nonzero scalars. To ensure that the resulting matrix is differentiable, we require a differentiable transition between B and C. To achieve this, [6] defines a nondecreasing $g : \mathbb{R} \to \mathbb{R}$, that obeys

$$g(t) = 0 \quad \forall\, t \leqslant 0 \tag{5.6}$$

$$g(t) = 1, \quad \forall\, t \geqslant 1, \text{ and} \tag{5.7}$$

$$g(t) \text{ is twice differentiable } \forall t. \tag{5.8}$$

An example of such a $g(t)$ is

$$g(t) = \begin{cases} \frac{1}{2}\left(1 - \cos\left(\pi t\right)\right) & 0 \leqslant t \leqslant 1 \\ 0 & t < 0 \\ 1 & t > 1. \end{cases} \tag{5.9}$$

Clearly, (5.9) satisfies (5.6) and (5.7). Further, (5.8) holds because

$$\lim_{t \to 0_+} \dot{g}(t) = \lim_{t \to 1_-} \dot{g}(t) = 0.$$

Now, for nonzero scalars b and c, we select $A(t)$ as follows. For a suitably small $\rho > 0$, define

$$\bar{T}_1 = \rho, \;\; \bar{T}_2 = \rho + \frac{\pi}{|b|}, \;\; \bar{T}_3 = 2\rho + \frac{\pi}{|b|}, \tag{5.10}$$

and

$$\bar{T}_4 = 3\rho + \frac{\pi}{|b|}, \;\; \bar{T}_5 = 3\rho + \frac{\pi}{|b|} + \frac{\pi}{|c|}, \;\; T_1 = \bar{T}_6 = 4\rho + \frac{\pi}{|b|} + \frac{\pi}{|c|}. \tag{5.11}$$

For all t, let $K_{T_1}(t)$ denote the largest integer k satisfying $t \geqslant kT_1$ and let $r_{T_1}(t) = t - K_{T_1}(t)T_1$. Then, [6] defines $A(t)$ as

$$A(t) = \begin{cases} g\left(\frac{r_{T_1}(t)}{\rho}\right) B & 0 \leqslant r_{T_1}(t) \leqslant \bar{T}_1 \\ B & \bar{T}_1 \leqslant r_T(t) \leqslant \bar{T}_2 \\ \left(1 - g\left(\frac{r_{T_1}(t) - \bar{T}_2}{\rho}\right)\right) B & \bar{T}_2 \leqslant r_{T_1}(t) \leqslant \bar{T}_3 \\ g\left(\frac{r_{T_1}(t) - \bar{T}_3}{\rho}\right) C & \bar{T}_3 \leqslant r_{T_1}(t) \leqslant \bar{T}_4 \\ C & \bar{T}_4 \leqslant r_T(t) \leqslant \bar{T}_5 \\ \left(1 - g\left(\frac{r_{T_1}(t) - \bar{T}_5}{\rho}\right)\right) C & \bar{T}_5 \leqslant r_{T_1}(t) \leqslant \bar{T}_6 \end{cases} \tag{5.12}$$

Then, we have the following theorem:

Theorem 5.2
Consider (3.2) with $A(t)$ and T_1, defined in (5.10)–(5.12). Then, for every pair of nonzero b, c, (v) of Assumption 3.2 holds.

Proof
Arguing as in the proof of Theorem 5.1, for every t, at least one of the following two cases holds:

Case 1: There is a contiguous interval of length $\pi/|b|$ in $[t, t + T_1]$, for which $\dot{\sigma}(t) = B\sigma(t)$ with B as in (5.4). Thus arguing similarly to the proof of Theorem 5.1 with suitable ξ_1 and scalar G_1, both dependent on t, and t_2 in this interval,

$$\dot{\sigma}(t_2) = G_1 \left[-\sin(bt_2 + \xi_1), \cos(bt_2 + \xi_1), 0\right]^\top.$$

DOI: 10.1002/acs

Then for every $\theta \in \mathbb{R}^3$, throughout this interval, $\theta^\top \dot{\sigma}(t_2)$ is a sinusoid of frequency b rad/sec. Thus, as this interval has length equalling half a cycle of such a sinusoid, $\theta^\top \dot{\sigma}(t_2)$ must become zero at least once in this interval.

Case 2: There is a contiguous interval of length $\pi/|c|$ in $[t, t+T_1]$, for which $\dot{\sigma}(t) = C\sigma(t)$ with C as in (5.5). Thus arguing similarly to the proof of Theorem 5.1 with suitable ξ_2 and scalar G_2, both dependent on t, and t_2 in this interval,

$$\dot{\sigma}(t_2) = G_2\,[0, -\sin(ct_2 + \xi_2), \cos(ct_2 + \xi_2)]^\top.$$

Then, for every $\theta \in \mathbb{R}^3$, throughout this interval, $\theta^\top \dot{\sigma}(t_2)$ is a sinusoid of frequency c rad/sec. Thus, as this interval has length equalling half a cycle of such a sinusoid, $\theta^\top \dot{\sigma}(t_2)$ must become zero at least once in this interval. □

6. SIMULATIONS

In this section, we provide the results of a set of simulation examples in $\mathbb{R}^3$ to demonstrate the performance of the adaptive localization and motion control scheme (2.2), (2.5),(2.6), (2.8), (3.1), (3.2), (5.4), (5.5) and (5.9)–(5.12). For comparison purposes, we consider the target settings in the examples of [5]. In all the examples, the design parameters and functions are selected as follows:

$$\begin{aligned} \alpha &= 1, \\ \gamma &= 10, \\ f(D) &= 1 - e^{-D}, \\ \beta &= 3, \\ b &= c = 1, \\ \rho &= 0.1, \\ \sigma(0) &= [0.6, 0.6, 0.6]^\top. \end{aligned}$$

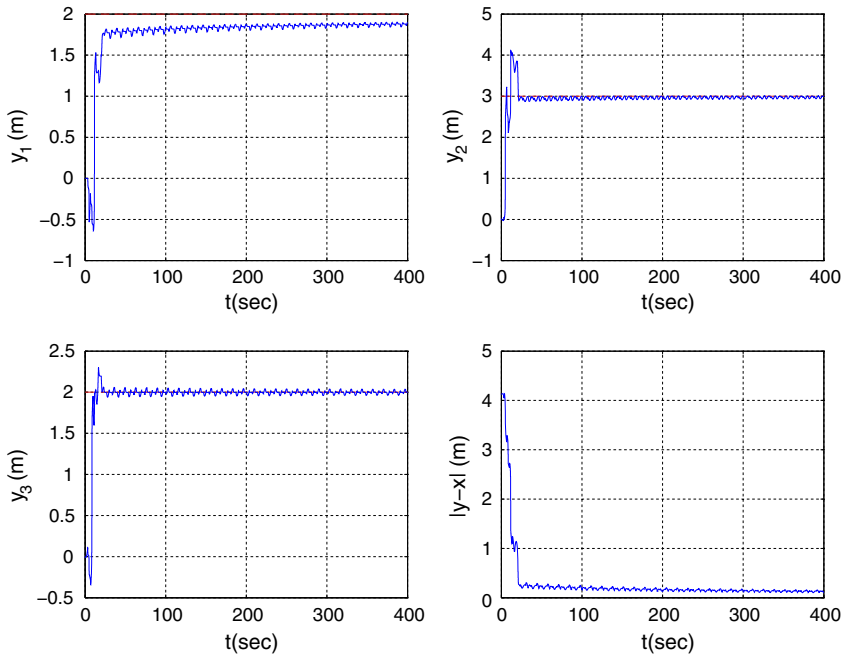

Figure 1. Agent motion for Example 1. The dashed lines correspond to the actual coordinates of the target T, and the solid curves show the trajectories of the mobile agent A.

DOI: 10.1002/acs

Example 1: The target is stationary, located at $x = [2, 3, 2]^\top$ (m). Using the adaptive scheme, we obtain the results shown in Figure 1. As can be seen in Figure 1, the agent successfully converges to the target location.

Example 2: This example is intended to test the robustness of the adaptive scheme to slow but persistent drifts in the target location. The target is moving around a nominal location at $x_n = [2, 3, 2]^\top$ (m) and its trajectory is given by $x(t) = [2 + \sin 0.005t,\ 3 + \cos 0.005t,\ 2]^\top$ (m).

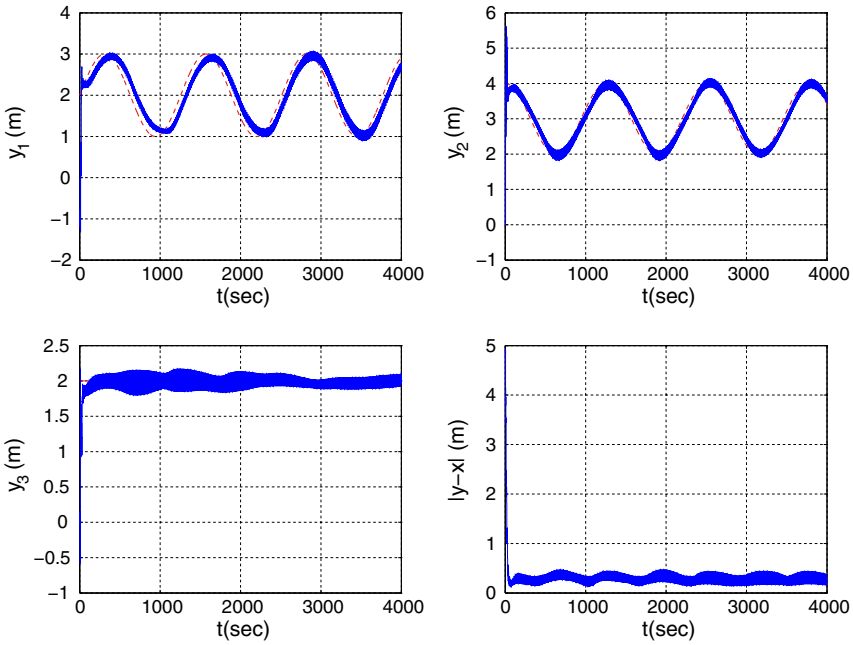

Figure 2. Agent motion for Example 2 for $t \in [0, 4000]$ (sec). The dashed lines correspond to the actual coordinates of the target T, and the solid curves show the trajectories of the mobile agent A.

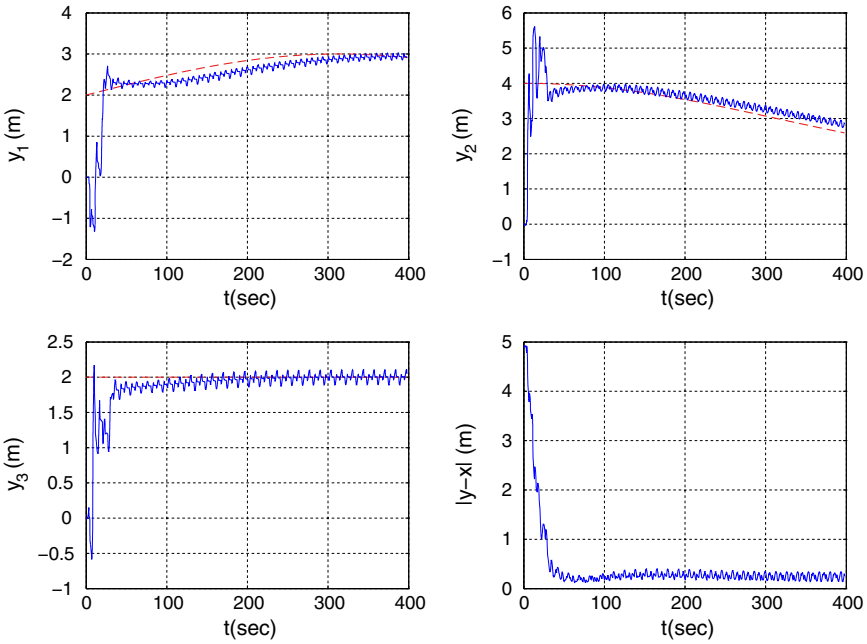

Figure 3. Agent motion for Example 2 for $t \in [0, 400]$ (sec). The dashed lines correspond to the actual coordinates of the target T, and the solid curves show the trajectories of the mobile agent A.

DOI: 10.1002/acs

Observe that the net extent of the drift in the first two coordinates is 2, and thus substantial. The rate of drift ($\dot{x}$), on the other hand, is relatively small having an amplitude of 0.005.

For this example, using the adaptive scheme, we obtain the results shown in Figure 2, whereas Figure 3 provides a snapshot of the initial tracking. $y(t)$ tracks the motion of $x(t)$ with a small error.

Example 3: This example is similar to Example 2, but the target drift rate is ten times that of Example 2, that is, $x(t) = [2 + \sin 0.05t,\ 3 + \cos 0.05t,\ 2]^{\top}$ (m). Figure 4 shows the tracking behavior. As expected the tracking though still quite good is with correspondingly larger error.

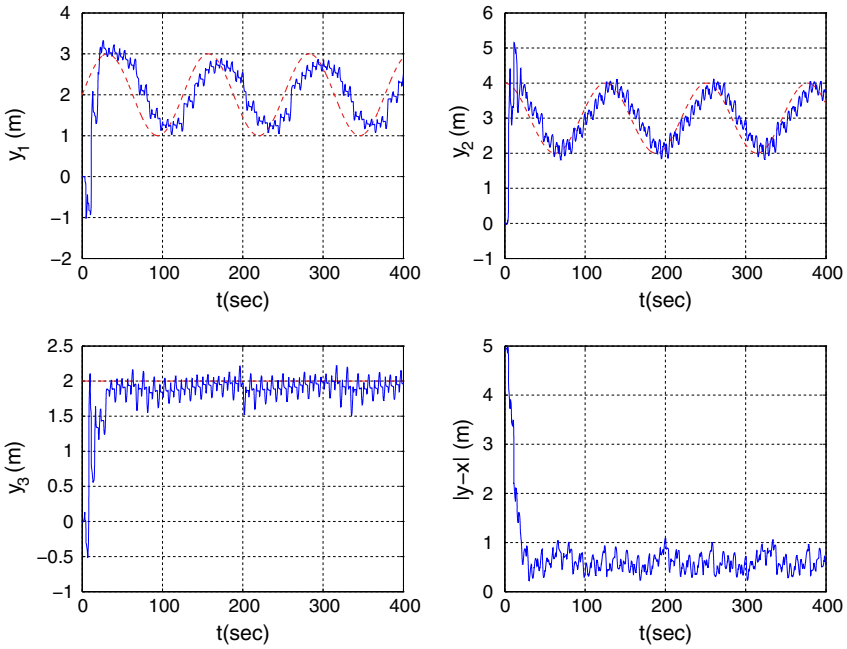

Figure 4. Agent motion for Example 3. The dashed lines correspond to the actual coordinates of the target T, and the solid curves show the trajectories of the mobile agent A.

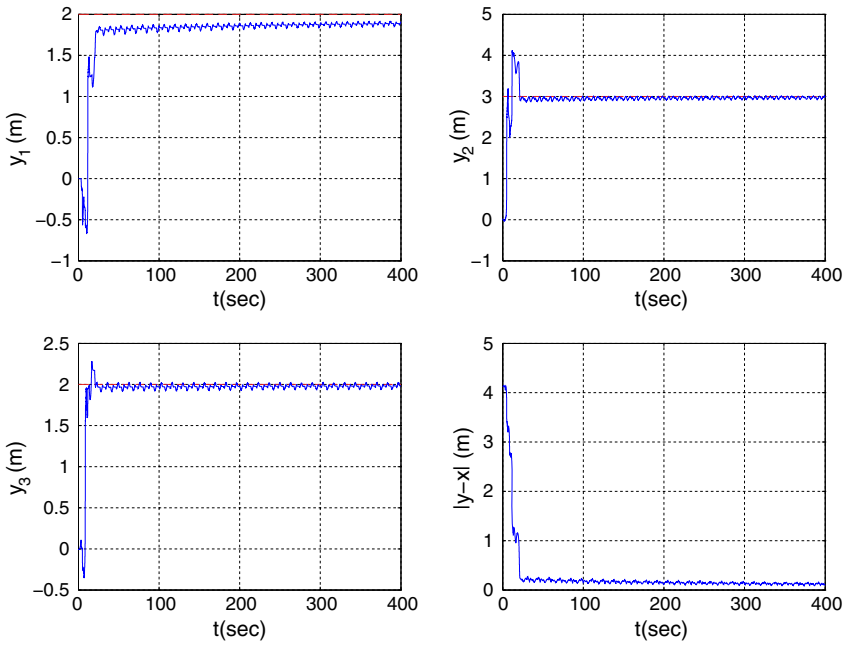

Figure 5. Agent motion for Example 4 with noise variance equal to 0.01 (m^2). The dashed lines correspond to the actual coordinates of the target T, and the solid curves show the trajectories of the mobile agent A.

DOI: 10.1002/acs

Example 4: Similar to Example 1, the target is stationary, located at $x = [2, 3, 2]^\top$ (m). In this example, we test noise performance, assuming that the distance measurement $D(t)$ is perturbed by a zero mean bandlimited white Gaussian noise. Figures 5 and 6, respectively, show the results with noise variances 0.01 (m^2) and 0.05 (m^2). (We would like to note that there is typo in the results shown in Figures 5, 6 and 8 of [5]; the noises variances for these figures ought to be 0.01, 0.05

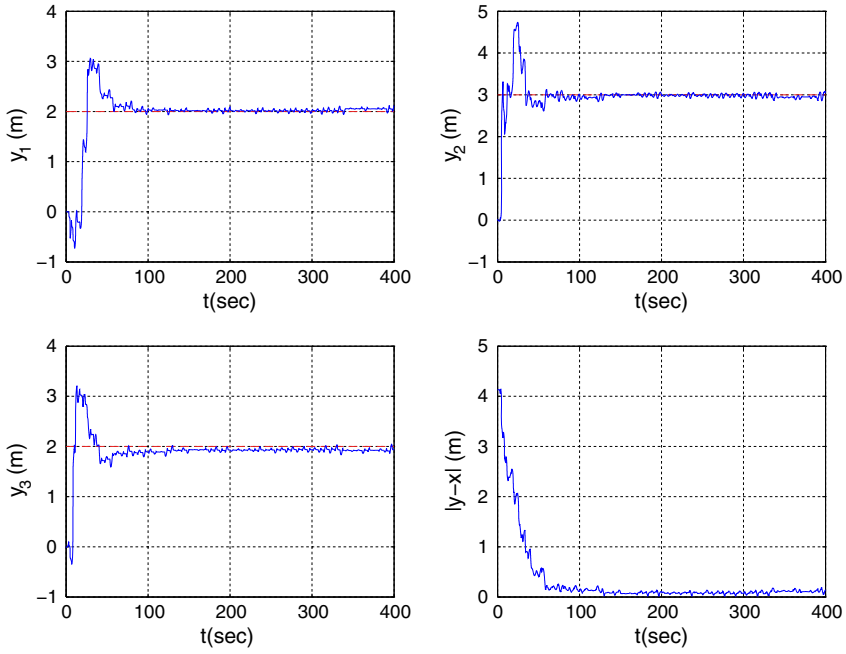

Figure 6. Agent motion for Example 4 with noise variance equal to 0.05 (m^2). The dashed lines correspond to the actual coordinates of the target T, and the solid curves show the trajectories of the mobile agent A.

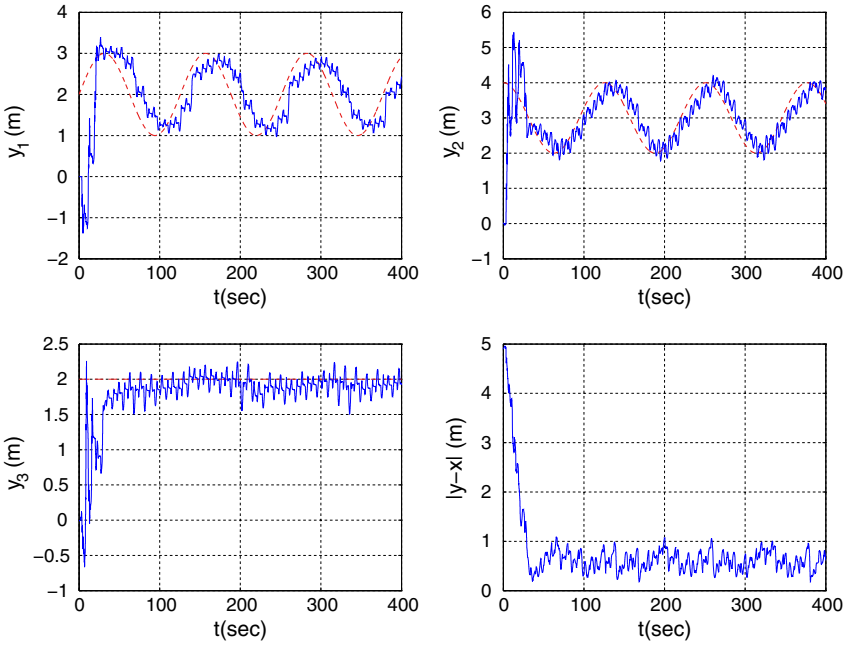

Figure 7. Agent motion for Example 5. The dashed lines correspond to the actual coordinates of the target T, and the solid curves show the trajectories of the mobile agent A.

DOI: 10.1002/acs

and 0.01, respectively, instead of 0.001, 0.005 and 0.001.) As can be seen in these figures, the agent successfully converges to the close vicinity of the target. As expected, the tracking error scales with the standard deviation of the noise.

Example 5: Similar to Example 3, the target is moving around a nominal location at $x_n = [2, 3, 2]^\top$ (m), and its trajectory is given by $x(t) = [2 + \sin 0.05t,\ 3 + \cos 0.05t,\ 2]^\top$ (m). For this drifting target case, we test noise performance, assuming that the distance measurement $D(t)$ is perturbed by a zero mean bandlimited white Gaussian noise with noise variance 0.01 (m^2). Figure 7 shows the results. As can be seen in Figure 1, the agent successfully converges to the close vicinity of the mobile target. The additional tracking error magnitude compared with Example 2 is of the magnitude of the measurement noise.

7. CONCLUSION

In this paper, we have presented the design of an adaptive scheme for localization of a target from distance measurements and motion control of a mobile agent to track and capture this target. The adaptive scheme is composed of a robust adaptive law that generates a location estimate of the target using distance measurements, and a motion control law that moves the mobile agent towards the estimated location in a way that provides the persistence of excitation needed for convergence of the location estimate of the target to the actual target location. A demonstration of stability with a convergence analysis for the overall adaptive control scheme is presented. The results are valid in both two and three dimensions of motion space. Simulation results are provided as well, demonstrating the performance of the proposed adaptive localization and motion control scheme as well as robustness of the scheme against slow bounded drifts in positions of the target and distance measurement noise.

As a follow-up study, the authors are currently working on extension of the design for cooperative target pursuit by a formation of autonomous agents. Other potential future works include formal analysis of the effects of target motion and robust modification of the proposed adaptive scheme to be compatible with mobile target cases.

REFERENCES

1. Bishop AN, Fidan B, Anderson BDO, Doğancay K, Pathirana PN. Optimality analysis of sensor-target localization geometries. *Automatica* March 2010; **46**(3):479–492.
2. Martinez S, Bullo F. Optimal sensor placement and motion coordination for target tracking. *Automatica* March 2006; **42**(4):661–668.
3. *IEEE Signal Processing Magazine* July 2005; **22**(4).
4. Mao G, Fidan B (eds). *Localization Algorithms and Strategies for Wireless Sensor Networks*. IGI Global - Information Science Publishing: Hershey, NY, 2009.
5. Dandach SH, Fidan B, Dasgupta S, Anderson BDO. A continuous time linear adaptive source localization algorithm robust to persistent drift. *Systems and Control Letters* 2009; **58**:7–16.
6. Shames I, Dasgupta S, Fidan B, Anderson BDO. Circumnavigation from distance measurements under slow drift. *IEEE Transactions on Automatic Control* 2012; **57**(4):889–903.
7. Shames I, Fidan B, Anderson BDO. Close target reconnaissance with guaranteed collision avoidance. *International Journal of Robust and Nonlinear Control* 2011; **21**(16):1823–1840.
8. Summers TH, Akella MR, Mears MJ. Coordinated standoff tracking of moving targets: control laws and information architectures. *AIAA Journal of Guidance, Control, and Dynamics* 2009; **32**(1):56–82.
9. Bopardikar SD, Bullo F, Hespanha JP. On discrete-time pursuit-evasion games with sensing limitations. *IEEE Transactions on Robotics* December 2008; **24**(6):1429–1439.
10. Kim T-H, Sugie T. Cooperative control for target-capturing task based on a cyclic pursuit strategy. *Automatica* 2007; **43**:1426–1431.
11. Bishop AN, Fidan B, Anderson BDO, Doğancay K, Pathirana PN. Optimal range-difference based localization considering geometrical constraints. *IEEE Journal of Oceanic Engineering* July 2008; **33**(3):289–301.
12. Bishop AN, Fidan B, Doğancay K, Anderson BDO, Pathirana PN. Exploiting geometry for improved hybrid AOA/TDOA based localization. *Signal Processing* July 2008; **88**(7):1775–1791.
13. Wigren T. A polygon to ellipse transformation enabling fingerprinting and emergency localization in GSM. *IEEE Transactions on Vehicular Technology* May 2011; **60**(4):1971–1976.

DOI: 10.1002/acs

14. Nagatani K, Ishida H, Yamanaka S, Tanaka Y. Three-dimensional localization and mapping for mobile robot in disaster environments. In *Proceedings of the IEEE/RSJ International Conference on Intelligent Robots and Systems*, Vol. 3, October 2003; 3112–3117.
15. Brennan SM, Mielke AM, Torney DC, Maccabe AB. Radiation detection with distributed sensor networks. *IEEE Computer* August 2004; **37**(8):57–59.
16. Howse JW, Ticknor LO, Muske KR. Least squares estimation techniques for position tracking of radioactive sources. *Automatica* November 2001; **37**(11):1727–1737.
17. Forman GH, Zahorzan J. The challenges of mobile computing. *IEEE Computer* April 1994:38–47.
18. Ioannou PA, Fidan B. *Adaptive Control Tutorial*. Society for Industrial and Applied Mathematics: Philadelphia, PA, 2006.
19. Ioannou PA, Sun J. *Robust Adaptive Control*. Prentice-Hall: Upper Saddle River, NJ, 1996.
20. Anderson BDO. Exponential stability of linear equations arising in adaptive identification. *IEEE Transactions on Automatic Control* May-June 1977:530–538.

DOI: 10.1002/acs